

Creative Commons Attribution 4.0 International (CC BY 4.0)

<https://creativecommons.org/licenses/by/4.0/>

Access to this work was provided by the University of Maryland, Baltimore County (UMBC) ScholarWorks@UMBC digital repository on the Maryland Shared Open Access (MD-SOAR) platform.

Please provide feedback


Please support the ScholarWorks@UMBC repository by emailing scholarworks-group@umbc.edu and telling us what having access to this work means to you and why it's important to you. Thank you.

Thermodynamics of Quantum Information in Noisy Polarizers

Maxwell Aifer^{1,*}, Nathan M. Myers^{2,†} and Sebastian Deffner^{1,‡}

¹*Department of Physics, University of Maryland, Baltimore, Maryland 21250, USA*

²*Department of Physics, Virginia Tech, Blacksburg, Virginia 24061, USA*

 (Received 12 December 2022; revised 14 April 2023; accepted 15 May 2023; published 15 June 2023)

Among the emerging technologies with prophesied quantum advantage, quantum communications has already led to fascinating demonstrations—including quantum teleportation to and from satellites. However, all optical communication necessitates the use of optical devices, the comprehensive quantum thermodynamic description of which is still severely lacking. In the present analysis, we prove several versions of Landauer’s principle for noisy polarizers, namely, absorbing linear polarizers and polarizing beam splitters. As main results, we obtain statements of the second law quantifying the minimal amount of heat that is dissipated in the creation of linearly polarized light. Our findings are illustrated with an experimentally tractable example, namely, the temperature dependence of a quantum eraser.

DOI: [10.1103/PRXQuantum.4.020343](https://doi.org/10.1103/PRXQuantum.4.020343)

I. INTRODUCTION

There are generally three applications in which quantum advantage is expected to be of technological significance—computation, sensing, and communication [1]. Despite the distinct and unique technological challenges of each area, devices designed for each of these applications can be considered as quantum devices that process information. Hence, they can be described by means of quantum thermodynamics [2].

The development of classical thermodynamics of information [3] originated in the formulation of Landauer’s principle [4]. This statement of the second law asserts that any computational task requiring the erasure of information must result in dissipation of heat and that the amount of heat produced is at least $k_B T \ln(2)$ times the number of logical bits erased. Recent years have seen intense research efforts in generalizing the bound to a wide variety of physical situations, such as classical systems with both discrete and continuous state spaces [5–9], as well as quantum systems undergoing Markovian and non-Markovian dynamics [10–13]. Landauer’s principle has even been experimentally verified in microscale systems using an overdamped colloidal particle in a double-well

potential [14]. However, given the rather heuristic nature of the original formulation [4], it is still being debated whether the original statement can really be shown in all generality [15–17]. Notably, some authors have recently interpreted certain non-Markovian processes as violations of Landauer’s principle [18–22].

Curiously, most of the current discussion is focused on statements of Landauer’s principle for computation. Yet, the communication of quantum information also obviously incurs thermodynamic costs, which can be determined with versions of the Landauer bound. Such “dynamical” formulations of Landauer’s principle can be traced back to Bremermann [23], who proposed that any computational device must obey the fundamental laws of physics, namely, *special relativity*, *quantum mechanics*, and *thermodynamics*. Then, identifying Shannon’s noise energy with the ΔE in Heisenberg’s uncertainty relation [24] for energy and time, $\Delta E \Delta t \geq \hbar$, he found an upper bound on the rate with which information can be communicated. A more rigorous argument has been put forward by Bekenstein [25] in the context of black-hole thermodynamics [26–30]. However, the Bremermann-Bekenstein bound does not seem to enjoy the same prominence as Landauer’s principle and, in fact, many different statements for the maximal rate with which entropy and information can be communicated have been formulated [31–44].

In the present work, we analyze the thermodynamics of some aspects of quantum optical communication. This is motivated by the fact that light is an attractive physical platform, given that it can carry information at the greatest possible speed and that it interacts relatively weakly with the environment [45,46]. The most significant technical challenge in creating optical quantum networks is

*maifer1@umbc.edu

†myersn1@vt.edu

‡deffner@umbc.edu

Published by the American Physical Society under the terms of the [Creative Commons Attribution 4.0 International](https://creativecommons.org/licenses/by/4.0/) license. Further distribution of this work must maintain attribution to the author(s) and the published article’s title, journal citation, and DOI.

to overcome attenuation [47,48]. Entanglement-swapping schemes can extend the range of quantum communication [49] but the performance of this method is still limited by the amount of dissipation caused by the individual optical components used [50–52]. Hence, a comprehensive thermodynamic characterization of noisy optical elements appears to be urgently needed. This perspective is in step with the recent attention given to studying the energetics of quantum information technologies [53].

Most communication schemes employ linearly polarized light [54]. Such light can be produced by sending unpolarized light through a linear polarizer, which absorbs one component of the electric field and transmits the component perpendicular to it. We call such optical elements absorbing linear polarizers (ALPs). It is also possible to produce linearly polarized light using a polarizing beam splitter (PBS), which transmits one component of the electric field and reflects the component that is perpendicular to it. While it is clear that some heat must be generated by the ALP, it is less obvious that there is any minimum amount of dissipation that is caused by the PBS [55,56]. In what follows, we show that both devices are, in fact, responsible for dissipation of heat when an assumption of locality is made, which can be understood through the concept of modularity dissipation [9].

Most light sources found in nature can be accurately described by the classical laws of electrodynamics and their description does not benefit from quantization of the field. However, there are engineered sources available that can produce single or entangled pairs of photons on demand and the results of experiments done with these sources cannot always be explained by classical electrodynamics [57–59]. In our analysis, we first address the case of classical light. The “classicality” of light can be characterized in a number of ways, such as by the negativity of the Wigner function [60,61]. For our purposes, we consider classical light to be a statistical mixture of approximate coherent states at large photon number. A derivation is given of a version of Landauer’s principle for ALPs acting on classical sources followed by a derivation of a similar result applicable to PBSs, assuming that the reflected light is inaccessible.

Next, we provide insight into more exotic sources with nonclassical behavior. We show that the findings for the PBS acting on classical light can be seen as stemming from local nonconservation of globally conserved quantities and that an analogous dissipation cost applies to quantum information-processing tasks. Having generalized the PBS result to the quantum case, we investigate the ALP acting on quantum sources and argue that an ALP can be modeled as a collection of PBSs strung together with intervening thermal reservoirs. Using this model, we are able to probe the dynamics of the polarization process, rather than just its end result. Interestingly, our model becomes formally equivalent to a repeated interaction scheme (or

collision model), which has received attention recently in the field of open quantum systems [62], including in the context of Landauer’s principle [63], and we leverage these existing results to quantify the dissipation that occurs as (possibly nonclassical) light propagates through the ALP. Notably, our analysis reveals a discontinuity in the slope of the energy-entropy curve as the temperature approaches zero, which agrees with previous investigations of the random scattering of light [64]. The collision-model approach also allows us to describe the dependence of the behavior of the ALP on its temperature, both in terms of optical extinction and decoherence. This permits us to make predictions concerning the relationship between temperature and the signature of entanglement observed in the quantum eraser [65–68]. We predict that at higher temperatures, the observed restoration of interference caused by measurement is suppressed.

II. LANDAUER’S PRINCIPLE FOR LINEAR POLARIZERS

In the following, we derive various statements of Landauer’s principle. The principle expresses that a decrease in Shannon entropy of an information-bearing degree of freedom is accompanied by the dissipation of heat [4,5,69]:

$$\mathrm{d}Q \geq k_B T (-ds), \quad (1)$$

where s is the differential Shannon entropy [70],

$$s = - \int dx f_X(x) \ln(f_X(x)). \quad (2)$$

Here, $f_X(x)$ denotes the probability density function (PDF) of a discrete or continuous random variable X .

In our case, X is the electric field, in which information is encoded. Then, an ALP has the effect of erasing this information stored in one component of the electric field. Therefore, by Landauer’s principle, the ALP should be required to dissipate heat. This is, in fact, the case and we now provide the corresponding statement of Landauer’s principle.

A. Classical absorbing linear polarizer

The ALP transmits horizontally polarized light and absorbs vertically polarized light. Consider a single mode of the electric field of frequency ω . The vertical component of the electric field is [71]

$$E_v(z, t) = iE_{0\omega} [\alpha_v(\omega) e^{i(\omega t - kz)} - \alpha_v^*(\omega) e^{i(kz - \omega t)}], \quad (3)$$

where the complex amplitude $\alpha_v(\omega)$ is considered a random variable with PDF f_α and $E_{0\omega}$ is an arbitrary constant electric field strength. The distribution is assumed to have

finite variance (and therefore finite energy) but is otherwise unspecified. The differential Shannon entropy of $\alpha_v(\omega)$ is

$$s[\alpha_v(\omega)] = - \int d^2\alpha_v f_\alpha(\alpha_v) \ln(f_\alpha(\alpha_v)), \quad (4)$$

where the integral is over the entire complex plane. We assume that the field decays rapidly outside of some region with volume V and so the ensemble-averaged energy content of the vertical component of the field is

$$E = \frac{1}{2} V \epsilon_0 E_{0\omega}^2 \langle |\alpha_v|^2 \rangle. \quad (5)$$

After the light has passed through the polarizer, in the simplest idealized scenario, all of the light that was initially present in the vertical mode of the electric field will have been absorbed. However, if the polarizer is at some finite temperature, there will still be light in the vertical mode due to thermal emission from the material. We address this idealized case here—in other words, ignoring other external sources of light and assuming that the polarizer absorbs all of the light that was in the vertical mode initially, replacing it with some thermal radiation. Therefore, we assume that the state of the field afterward is a thermal state, given by the canonical ensemble, $f^{\text{can}} \propto \exp(-E/k_B T_P)$, where T_P is the temperature of the polarizer. Although it is well known that this assumption leads to an infinite total energy in the completely classical case when all frequencies are present [72], this does not affect the present argument, which only concerns a single mode of the field. This thermal state has entropy s^{can} and so the total erasure is simply the difference,

$$-\Delta s = s - s^{\text{can}}. \quad (6)$$

We show in Appendix A that the following statement of Landauer's principle holds:

$$Q \geq k_B T_P (e^{-\Delta s} - 1). \quad (7)$$

Expanding about zero for small Δs , we obtain the Landauer bound

$$dQ \geq k_B T_P (-ds). \quad (8)$$

Equations (7) and (8) are our first main results, asserting Landauer's principle for the ALP. The assumption of finite variance of the field is necessary to avoid having a divergent amount of heat dissipated and, similarly, it is necessary to assume that the ALP does not perfectly polarize the field (a thermal distribution at temperature T_P remains in the vertical component) to avoid a divergent change in differential entropy. The assumption that all energy is converted to heat is justified on the basis that

the ALP is a passive component, with no mechanism for storing energy. If there are multiple frequencies ω_j in the source, we may treat the amplitude at each frequency as a random variable $\alpha_v(\omega_j)$ and we assume that these are not correlated with each other. In this case, due to the additivity of the Shannon entropy and the energy, the same result holds (in fact, this argument holds even for a continuum of modes). We leave the case of correlated amplitudes for future work. It should also be noted that the quantity $-ds$ should not be interpreted as an amount of data that is erased but simply as a decrease in the Shannon entropy. There is a subtle distinction between these concepts, given that it is possible that there is still some finite Shannon entropy even if all of the original data have been erased, if the original content of the signal has been replaced by random thermal fluctuations.

B. Quantum absorbing linear polarizer

The somewhat natural question is how things change if the light is treated quantum mechanically. In the quantum case, the amplitude α is no longer an observable and thus it does not have a probability density function. Instead, we consider the dimensionless quadratures [73]

$$\hat{q} = \frac{1}{\sqrt{2}} (\hat{a}^\dagger + \hat{a}) \quad (9)$$

and

$$\hat{p} = \frac{i}{\sqrt{2}} (\hat{a}^\dagger - \hat{a}), \quad (10)$$

in terms of which the Hamiltonian is expressed as

$$\hat{H} = \frac{1}{2} \hbar \omega (\hat{q}^2 + \hat{p}^2). \quad (11)$$

Therefore, the average energy is

$$E = \frac{1}{2} \hbar \omega (\langle q^2 \rangle + \langle p^2 \rangle). \quad (12)$$

Since \hat{q} and \hat{p} do not commute, the interpretation of a joint probability distribution over these variables is ambiguous, so it is not immediately clear how to define the entropy.

Especially in quantum optics [73], it has proven particularly useful to express quantum states in their Wigner representation,

$$W(q, p) = \frac{1}{\pi \hbar} \int dy \langle q + y | \rho | q - y \rangle e^{-2ip y / \hbar}. \quad (13)$$

Correspondingly, a Wigner entropy can be defined as [74]

$$s_W[W] = - \int dq dp W(q, p) \ln(W(q, p)), \quad (14)$$

which is simply the Weierstrass transform of the Wehrl entropy. The latter has been shown to be thermodynamically significant [75]. However, the Wigner entropy is only defined for states with strictly positive Wigner functions. Nonetheless, we are able to define a “maximal Wigner entropy” for arbitrary states by the following argument: the subadditivity of classical Shannon entropy dictates that for a joint distribution $f_{X,Y}$ with marginal distributions f_X and f_Y [76],

$$s[f_{X,Y}] \leq s[f_X] + s[f_Y]. \quad (15)$$

When the Wigner entropy is defined, it is the same as the Shannon entropy over a joint distribution. Also, recall that the marginals of the Wigner distribution are the distributions for the quadratures q and p [73]. Therefore, the following subadditivity rule is obeyed:

$$s_W[W] \leq s[f_q] + s[f_p]. \quad (16)$$

Even when $s_W[W]$ is not defined, we can still evaluate $s[f_q]$ and $s[f_p]$ and we define the maximal Wigner entropy as

$$s_{WM}[W] = s[f_q] + s[f_p]. \quad (17)$$

Then, erasure is bounded above by

$$-\Delta s_W \leq s_{WM}[W] - s_W[W']. \quad (18)$$

It is shown in Appendix B that the following version of Landauer’s principle holds:

$$Q \geq \frac{\hbar\omega}{2} \coth\left(\frac{\hbar\omega}{2k_B T}\right) (e^{-\Delta s_W} - 1). \quad (19)$$

Again, expanding for small Δs , we have

$$\mathfrak{d}Q \geq \coth\left(\frac{\hbar\omega}{2k_B T}\right) (-ds_W), \quad (20)$$

Note that we once again assume that the vertical mode is in a thermal state after the light has passed through the polarizer, although this time it is the corresponding quantum canonical ensemble state. The grounds for this assumption are much the same as in the classical case; this is what we would expect for an idealized ALP that completely transmits the horizontal mode and completely absorbs the vertical mode, when there are no other external light sources present. In Fig. 1, we plot the two Landauer bounds given in Eqs. (8) and (20) as a function of the temperature. Observe that they agree at high temperatures and at low temperature (when $\hbar\omega \approx k_B T$), the quantum heat cost per bit asymptotically approaches a constant value $\ln(2)/2$, while the classical heat cost per bit goes to zero.

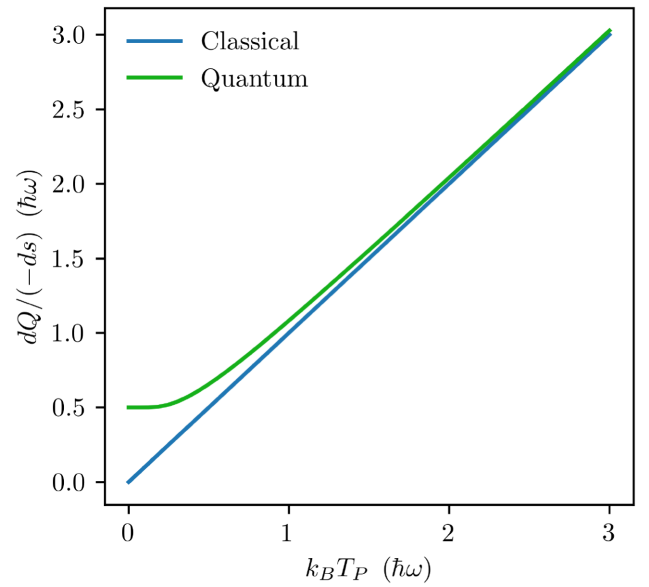


FIG. 1. A comparison of the classical [Eq. (8)] and quantum [Eq. (20)] Landauer bounds for the ALP.

III. LANDAUER’S PRINCIPLE FOR POLARIZING BEAM SPLITTERS

Another optical element that is subject to dissipation is the PBS. Note that it is possible to produce linearly polarized light with a PBS, which transmits horizontally polarized light and reflects vertically polarized light in a different direction. In this case, rather than being absorbed, the vertically polarized output is simply sent elsewhere (cf. Fig. 2). It is not clear that there is any nonzero amount of heat that must be generated in this process, which is often assumed to be nondissipative [77]. In what follows, we show that there is a minimal amount of dissipation that scales with temperature.

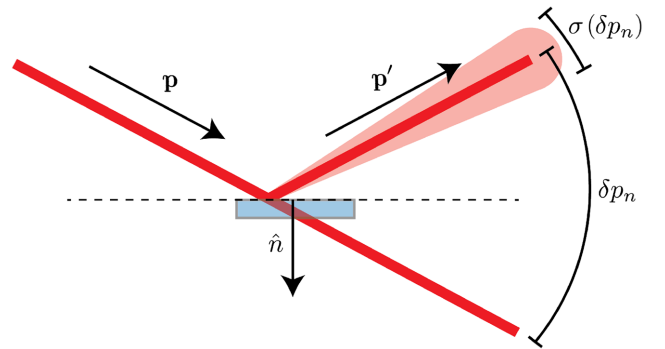


FIG. 2. A schematic representation of a PBS. The incident beam is separated into its horizontal and vertical polarization components.

A. Semiclassical description

We first treat the PBS semiclassically, meaning that we do not involve the quantum state of light, although we consider it to be made up of pointlike particles; in other words, we are using the Newtonian corpuscular model [78]. Each photon is assumed to have either horizontal or vertical polarization, with the polarization of each photon an independent random variable, and to have probability 1/2 of being vertically polarized and probability 1/2 of being horizontally polarized. The PBS itself is assumed to have mass m and temperature T and the photons are assigned a frequency $\omega = E/\hbar$. In Appendix C, we analyze the effect of sending many such photons in sequence through the PBS, which we find results in the dissipation of heat. Some details from the derivation are included here to clarify the way in which heat arises in our treatment.

As in Fig. 2, let \hat{n} be the unit vector, which is perpendicular to the PBS surface and is pointing *into* the bulk. The PBS and the photon have momenta \mathbf{p}_b and \mathbf{p} , respectively, in the laboratory frame. We define $p_{bn} = \hat{n} \cdot \mathbf{p}_b$ and $p_n = \hat{n} \cdot \mathbf{p}$ as the inward normal components of \mathbf{p}_b and \mathbf{p} . Evidently, for momentum to be conserved, if the photon is reflected, then some momentum kick must be imparted to the PBS. For a PBS traveling at nonrelativistic speed with macroscopic mass, we find that the conservation of momentum can be expressed as

$$\delta p_n = -2p_n + 2\hbar\omega p_{bn}/mc^2, \quad (21)$$

where δp_n is the \hat{n} component of the difference in momentum between the reflected and transmitted photons. It is then assumed that the momentum of the PBS is drawn from a canonical distribution at temperature T , i.e.,

$$p_{bn} \sim \mathcal{N}(0, mk_B T). \quad (22)$$

Each incident photon can be viewed as a Bernoulli trial, with a probability of 1/2 of imparting a momentum change δp to the PBS, resulting in a binomial distribution for the total change in momentum after N photons have arrived:

$$\frac{p_{bn}(t) - p_{bn}(0)}{\delta p_{bn}} \sim B(N, 1/2). \quad (23)$$

In the limit of many photons, we see that the momentum is still canonically distributed but the width of the momentum distribution is increased, so it is effectively at a higher temperature, which we interpret as resulting from the dissipation of heat.

One might then try to minimize the momentum kick imparted to the beam splitter by sending the photon in at a very small angle of incidence. However, as the PBS itself has an uncertain momentum, this causes the direction of the reflected photon to become uncertain and this uncertainty must not be greater than the difference in mean

momentum between the two paths or it will be impossible to distinguish reflected photons from transmitted photons. That is, we write

$$|\langle \delta p_n \rangle| \geq \sigma[\delta p_n]. \quad (24)$$

Finally, the information content of the independent identically distributed (IID) sequence of photon polarizations is simply 1 bit per photon and we associate this information content with the information change in Landauer's principle. As a consequence of the above considerations, which are elaborated on in detail in Appendix C, under the assumption that the reflected photons are locally unavailable, the following lower bound on dissipation holds:

$$\mathfrak{d}Q \geq \frac{\hbar^2 \omega^2}{2m^2 c^4} k_B T (-ds). \quad (25)$$

Equation (25) relates the logical information processed to the dissipation cost for the semiclassical PBS. This result is similar to Landauer's principle in that it is a lower bound on heat generation that is proportional to the amount of logical information processed. However, it differs in that it does not require any information to be “erased” *per se*. In our treatment, we assume that light that is reflected by the beam splitter is no longer accessible locally, which leads to dissipation. This is an instance of the more general phenomenon of modularity dissipation [9], whereby locally accessible information is transformed into global correlations across different parts of a system, which cannot be exploited due to physical constraints.

B. Quantum nonconservation cost

The result of Sec. II A is based on the global conservation of momentum and on the assumption of modularity, which prevents the exploitation of global correlations. This reasoning can be generalized to any information-processing scheme that locally does not conserve quantities that are globally conserved, even if the desired logical operation is invertible. Here, we give an example of this nonconservation cost in a quantum system that is equivalent to the PBS.

Consider the action of the PBS in the one-photon subspace. The basis states of this subspace are

$$|h1\rangle, |h2\rangle, |v1\rangle, |v2\rangle. \quad (26)$$

With this basis ordering, the PBS unitary is then given by the following matrix:

$$U_{\text{PBS}} = \begin{pmatrix} 1 & 0 & 0 & 0 \\ 0 & 1 & 0 & 0 \\ 0 & 0 & 0 & 1 \\ 0 & 0 & 1 & 0 \end{pmatrix}. \quad (27)$$

The PBS can therefore be thought of as a controlled-NOT (CNOT) operation action on a two-qubit system, the control

qubit of which is the polarization degree of freedom and the target degree of freedom of which is the path, $U_{\text{PBS}} = U_{\text{CN}}$, for the one-photon subspace [79]. However, since the components of angular momentum are globally conserved, it is not possible to implement this operation deterministically unless there is access to a bath that can absorb the change in angular momentum. It has been realized that global conservation laws constrain the possible fidelity of quantum gates [80,81], although to our knowledge this has not been applied to finding the thermodynamic cost of quantum gates under an assumption of modularity.

We assume that the two-qubit register and the bath are initially separable. The target qubit is known to be in the zero state, the control qubit is in the completely mixed state, and the bath is in an arbitrary state

$$\rho = \frac{1}{2}(|0\rangle\langle 0| + |1\rangle\langle 1|) \otimes |0\rangle\langle 0| \otimes \rho_B, \quad (28)$$

where the bath is a register of N qubits. As it is not possible to actually implement the CNOT exactly, by the previous arguments, we assume that it is implemented with some error bound ϵ . This is similar to the C-maybe interaction that has been studied in the context of quantum Darwinism [82–84]. Explicitly, we have

$$\sqrt{\text{tr} \left\{ \left(\rho'_S - U_{\text{CN}} \rho_S U_{\text{CN}}^\dagger \right)^2 \right\}} \leq \epsilon. \quad (29)$$

We show in Appendix D that the loss of purity on the bath is bounded below by

$$\text{tr} \{ \rho_B'^2 \} \leq \text{tr} \{ \rho_B^2 \} - \frac{1}{N2^N} \left(1 - 2\sqrt{2}\epsilon \right)^2. \quad (30)$$

This implies that for error $\epsilon < (2\sqrt{2})^{-1}$, there is a nonzero loss of purity on the bath as a result of the CNOT operation and the minimal loss of purity decreases exponentially with the size of the bath.

Figure 3 gives a comparison of the bounds given by Eqs. (25) and (30), plotted as a function of the system size. It is assumed that in the quantum case, the register is made up of electrons, so the number of spins is simply m/m_e . However, the two equations give lower bounds on the change in different quantities (heat and purity), so they cannot be compared directly. We still may get an idea of how the order of magnitude of the quantum and classical bounds compare at different system sizes. The plot shows that for $m/m_e > 100$, the classical bound dominates and for $m/m_e < 100$, the quantum bound becomes more relevant.

IV. QUANTUM MASTER EQUATION FOR LINEAR POLARIZERS

The above analysis makes it apparent that a more rigorous treatment of optical elements as genuinely quantum

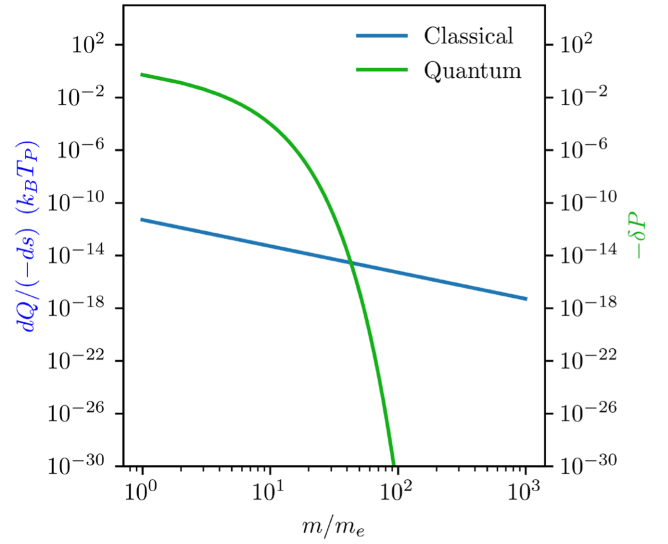


FIG. 3. A comparison of the classical [Eq. (25)] and quantum [Eq. (30)] dissipation bounds for the PBS.

devices is required. To this end, we now consider the propagation of light through an ALP and model this as a dynamical process using a quantum master equation. The ALP is conceptualized as a series of layers through which the light propagates, interacting with each layer in turn (see Fig. 4). Each layer is modeled as a PBS, which allows for noise photons to enter from the environment as well as for losses of photons to the environment due to attenuation. To

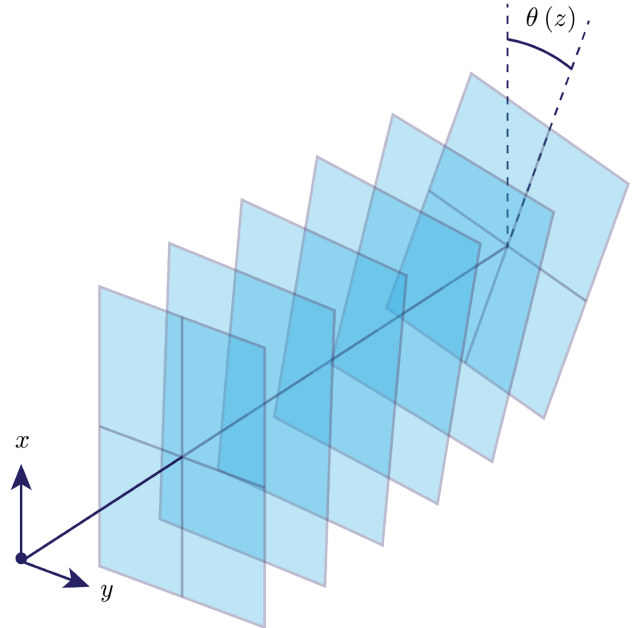


FIG. 4. A polarizer conceptualized as a sequence of planes with varying polarization axes.

set up this model, we first give the quantum description of the PBS.

A. Quantum polarizing beam splitter

The PBS has two input ports, each with two polarization modes. We label the two polarization modes of one input port a_h and a_v and, similarly, use b_h and b_v for the other input port (these later become the annihilation operators for the input ports). The corresponding output ports are labeled a'_h , a'_v , b'_h , and b'_v (see Fig. 5).

The behavior of the PBS is easily described in the Heisenberg picture, where the operators are transformed by a scattering matrix S :

$$\begin{pmatrix} a'_h \\ a'_v \\ b'_h \\ b'_v \end{pmatrix} = S \begin{pmatrix} a_h \\ a_v \\ b_h \\ b_v \end{pmatrix}. \quad (31)$$

The PBS scattering matrix for the PBS may be taken to be

$$S = \begin{pmatrix} 1 & 0 & 0 & 0 \\ 0 & t & 0 & r \\ 0 & 0 & 1 & 0 \\ 0 & -r & 0 & t \end{pmatrix}, \quad (32)$$

where t and r are the transmission and reflection coefficients, satisfying $t^2 + r^2 = 1$. We therefore use the parametrization $t = \cos(\phi)$, $r = \sin(\phi)$. We can also describe PBS the transmission and reflection axes of which are rotated by an angle θ . In this case, the scattering matrix

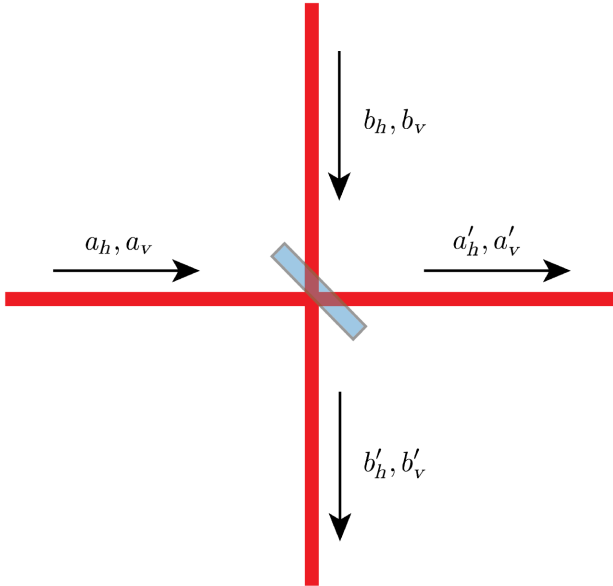


FIG. 5. The port-labeling convention for the PBS.

is

$$S_\theta = R_\theta S R_\theta^\dagger, \quad (33)$$

where

$$R_\theta = \begin{pmatrix} \cos(\theta) & -\sin(\theta) & 0 & 0 \\ \sin(\theta) & \cos(\theta) & 0 & 0 \\ 0 & 0 & \cos(\theta) & -\sin(\theta) \\ 0 & 0 & \sin(\theta) & \cos(\theta) \end{pmatrix}. \quad (34)$$

As is shown in Appendix F, the Schrödinger-picture evolution operator on the Hilbert space of quantum states can be evaluated as

$$U = \exp \left(\sum_{ij} \ln(S)_{ij} a_i^\dagger a_j \right). \quad (35)$$

In this case, we find

$$U(\theta, \phi) = \exp \left(\phi [\sin^2(\theta) S_h + \cos^2(\theta) S_v + \sin(2\theta) S_c] \right), \quad (36)$$

where

$$S_h = a_h^\dagger b_h - b_h^\dagger a_h, \quad (37)$$

$$S_v = a_v^\dagger b_v - b_v^\dagger a_v, \quad (38)$$

and

$$S_c = \frac{1}{2} (b_v^\dagger a_h + b_h^\dagger a_v - a_v^\dagger b_h - a_h^\dagger b_v). \quad (39)$$

The density matrix is then transformed by a unitary map

$$\rho' = U(\theta, \phi) \rho U^\dagger(\theta, \phi). \quad (40)$$

Finally, the quantum state exiting the PBS is given formally by

$$\rho' = F_\theta(\rho) = \text{tr}_b \left\{ U_\theta \rho \otimes \eta_T U_\theta^\dagger \right\}, \quad (41)$$

where η_T is the Gibbs state at the temperature T of the environment.

B. Multilayer model of the linear polarizer

We model the linear polarizer as a sequence of PBS elements at randomized angles, which are drawn from a thermal distribution (see Fig. 6). These PBS elements represent physical objects (e.g., the nanoparticles in a nanoparticle-based polarizer), which are in uncertain configurations due to thermal energy. Initially, the system is in

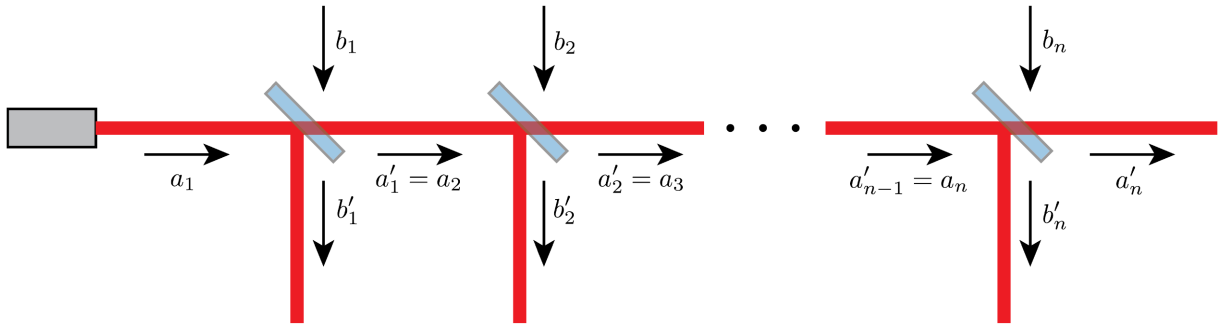


FIG. 6. A linear polarizer modeled as a chain of PBSs.

some mixed state ρ_0 of the form of Eq. (47). At each layer, the state is transformed using Eq. (41). We also allow the angle of each polarizer to be different, so the n th step of the evolution is given by

$$\rho_{n+1} = \text{tr}_{\text{b}_n} \{ U_n \rho_n \otimes \eta_T U_n^\dagger \} = F_n(\rho_n). \quad (42)$$

Equation (42) is of the form of a so-called collision model or repeated-interaction scheme [62,85,86].

We see from Eq. (36) that there is a continuum limit as long as ϕ is taken to zero as dt goes to zero. We set $\phi = c_\phi dt$. Then, to first order in dt , we have

$$U_\theta = 1 + c_\phi dt (\sin^2(\theta) S_h + \cos^2(\theta) S_v + \sin(2\theta) S_c). \quad (43)$$

This leads to the following master equation:

$$\frac{d\rho}{dt} = c_\phi \text{tr}_{\text{b}} \{ [\mathcal{H}_\theta, \rho \otimes \eta_T] \}, \quad (44)$$

where

$$\mathcal{H}_\theta = \sin^2(\theta) S_h + \cos^2(\theta) S_v + \sin(2\theta) S_c. \quad (45)$$

It has been shown by Lorenzo *et al.* [11] that for collision models of this form, the following form of Landauer's principle is observed:

$$\text{d}Q \geq k_B T (-ds), \quad (46)$$

which is again the desired result.

C. Single-photon states at low temperature

To make contact with experimentally realistic scenarios, we are concerned with photons of optical frequency (approximately 10^{14} Hz), so at room temperature ($k_B T \approx 25$ meV) the probability of finding n photons in a given mode is proportional to $\exp(-17n)$. We therefore assume that the number of photons in the vacuum ports is always 0 initially. We are effectively treating the environment as

being at zero temperature for the purposes of thermal radiation. However, we do not assume zero temperature for the mechanical degrees of freedom of the polarizer itself, which contribute to uncertainty in the transmission axis.

Suppose that incident on the input port of a PBS there is a general mixed state belonging to the subspace with at most one photon:

$$\rho = \sum_{\alpha, \alpha' \in \{0, h, v\}} c_{\alpha\alpha'} |\alpha\rangle \langle \alpha'|. \quad (47)$$

The state of the two input ports a and b combined is then

$$\sigma = \rho \otimes |0\rangle \langle 0|. \quad (48)$$

We are concerned with the reduced density matrix for the input mode, ρ . The evolution of ρ is given by

$$\rho' = \text{tr}_{\text{b}} \{ U_\theta \rho \otimes |0\rangle \langle 0| U_\theta^\dagger \}. \quad (49)$$

The evolution given by Eq. (41) is a completely positive trace-preserving (CPTP) map [87] and therefore can be given in terms of Kraus operators. For this particular case, it can be expressed in terms of two Kraus operators that depend on θ , $K_{1\theta}$ and $K_{2\theta}$:

$$\rho' = F_\theta(\rho) = K_{1\theta}^\dagger \rho K_{1\theta} + K_{2\theta}^\dagger \rho K_{2\theta}. \quad (50)$$

Explicitly, the Kraus operators are

$$K_{1\theta} = \begin{pmatrix} 1 & 0 & 0 \\ 0 & t \cos^2(\theta) + \sin^2(\theta) & -(1-t) \sin(\theta) \cos(\theta) \\ 0 & -(1-t) \sin(\theta) \cos(\theta) & \cos^2(\theta) + t \sin^2(\theta) \end{pmatrix} \quad (51)$$

and

$$K_{2\theta} = \begin{pmatrix} 0 & r \cos(\theta) & r \sin(\theta) \\ 0 & 0 & 0 \\ 0 & 0 & 0 \end{pmatrix}. \quad (52)$$

Equations (50), (51), and (52) completely specify the evolution of the density matrix as the single photon propagates

through a single layer of the polarizer at low temperature. To simulate the evolution in the multilayer model, the angle θ for each polarizer is drawn from a thermal distribution,

$$f(\theta) = \frac{1}{\sqrt{2\pi k_B T/\kappa}} \exp\left(-\frac{1}{2} \frac{\theta^2}{k_B T/\kappa}\right), \quad (53)$$

where κ is a physical parameter of the polarizing material that characterizes the energy required to change the orientation of polarizing elements from their (mechanical) equilibrium positions. The resulting maps F_θ are applied one after another. For $\theta = 0$, we obtain a particularly simple evolution:

$$F_0(\rho) = \begin{pmatrix} \rho_{00} + r^2 \rho_{11} & t \rho_{01} & \rho_{02} \\ t \rho_{10} & t^2 \rho_{11} & t \rho_{12} \\ \rho_{20} & t \rho_{21} & \rho_{22} \end{pmatrix}. \quad (54)$$

In Appendix E, we consider the Heisenberg-picture description of a single application of the map F_θ with a random angle drawn from the distribution given in Eq. (53). It is found that an adjoint map can be defined that gives evolved operators satisfying a modified commutation relation,

$$[a'_h, a'^{\dagger}_h] = [a'_v, a'^{\dagger}_v] = 1 - 2(1-t)(\chi - \chi^2), \quad (55)$$

where $\chi = 1/2[1 - \exp(-2k_B T/\kappa)]$.

In Eq. (55), we observe the direct impact of the noise in the PBS on the optical signal. The quantum mechanical commutation relations “degrade” as a function of temperature, which is simply another way of looking at effects of decoherence.

D. Numerical study of the low-temperature limit

Using the above formalism, we simulate the evolution of the quantum state of light, limited to the ≤ 1 -photon subspace and assuming low temperature, i.e., $k_B T \ll \hbar\omega$. This simulation allows us to discuss some qualitative aspects of the polarization process. We initialize the system in the state

$$\rho_0 = \begin{pmatrix} 1/3 & 1/3 & 1/3 \\ 1/3 & 1/3 & 1/3 \\ 1/3 & 1/3 & 1/3 \end{pmatrix}. \quad (56)$$

Then the CPTP map F_0 is iterated for $N = 10\,000$ layers with $t = 0.9$. A range of temperatures are chosen in the interval $\sqrt{k_B T/\kappa} \in [0.05, 0.3]$. We find that the population $p_v = \rho_{vv}$ decays very quickly, as expected, falling to near zero after < 100 layers. The horizontal population p_h takes a longer time to decay. As the temperature increases, p_v decays more slowly and p_h decays more quickly, until the two polarizations behave near identically for $\sqrt{k_B T/\kappa} \approx$

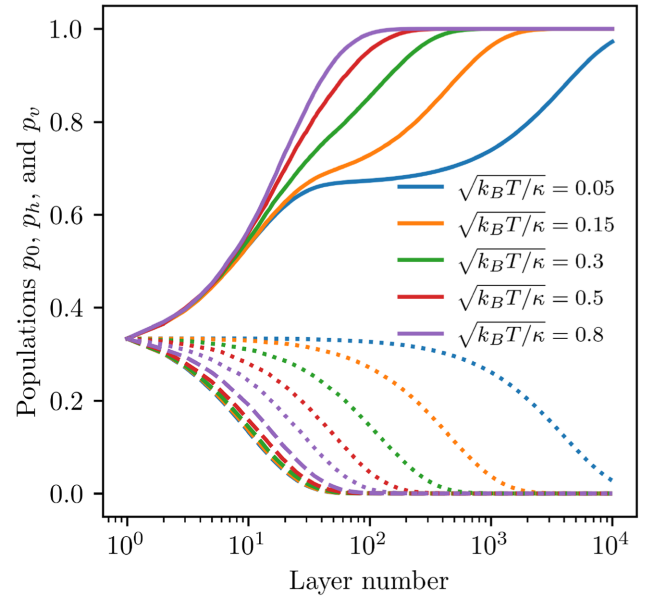


FIG. 7. The time dependence of the populations $p_0 = \rho_{00}$ (solid lines), $p_h = \rho_{11}$ (dotted lines), and $p_v = \rho_{22}$ (dashed lines). The vertical population p_v rapidly decays to zero but the horizontal component takes longer. As a result, the vacuum population has a plateau that is flatter at lower temperatures.

1. At low temperature, due to the lag between absorption of vertically and horizontally polarized light, the vacuum population has a plateau at intermediate times (see Fig. 7).

We see from Fig. 8 that the coherences $|\rho_{v0}|^2$ and $|\rho_{hv}|^2$ decay exponentially, with the horizontal-vacuum coherence decaying faster. The decay of coherence occurs faster at higher temperatures. This result is in line with our expectations, given that decoherence has been found to be enhanced at higher temperatures in a variety of physical systems [88–90].

The Shannon entropy is evaluated at all times and it is found to decrease monotonically. The energy is proportional to $1 - p_0$, and also decreases monotonically. Figure 9 shows the time dependence of the energy and the Shannon entropy, with both displaying the plateau feature at low temperatures discussed earlier.

Landauer’s principle concerns the change in heat relative to the change in Shannon entropy, which can be expressed as the derivative $dQ/(-ds)$ along a system trajectory. Since we assume that $dQ = -dE$, we are therefore interested in the derivative dE/ds along some system trajectory. Although this ratio is related to the temperature, it is not given by any function of the temperature, given that the system is out of equilibrium. We plot the energy against the Shannon entropy for 100 realizations of the random process at various temperatures. For each realization, the angles of the polarizer layers are drawn from a Boltzmann distribution at the given temperature and the initial conditions are always those given by Eq. (56).

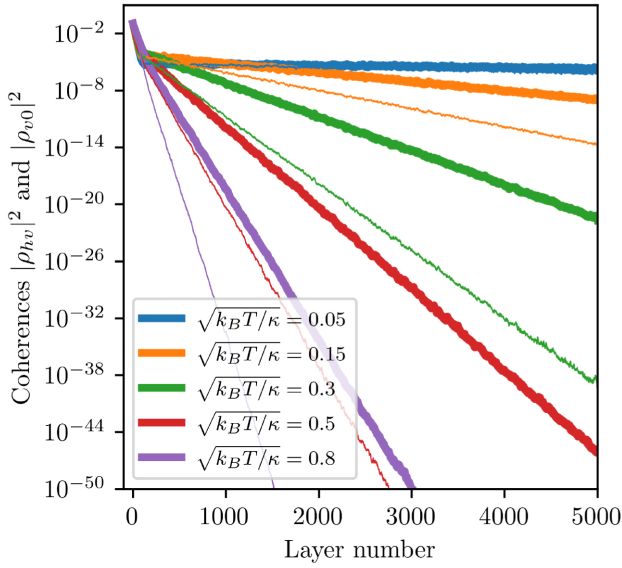


FIG. 8. The time dependence of the coherences $|\rho_{hv}|^2$ (thick lines) and $|\rho_{v0}|^2$ (thin lines). The coherences both decay exponentially but $|\rho_{v0}|^2$ decays at a faster rate at all temperatures. Both coherences decay faster at higher temperatures.

Figure 10 shows that the energy always increases monotonically with the Shannon entropy, as expected. Interestingly, as the temperature approaches zero, a discontinuity of the slope appears near $s = 0.6$. This can be explained by

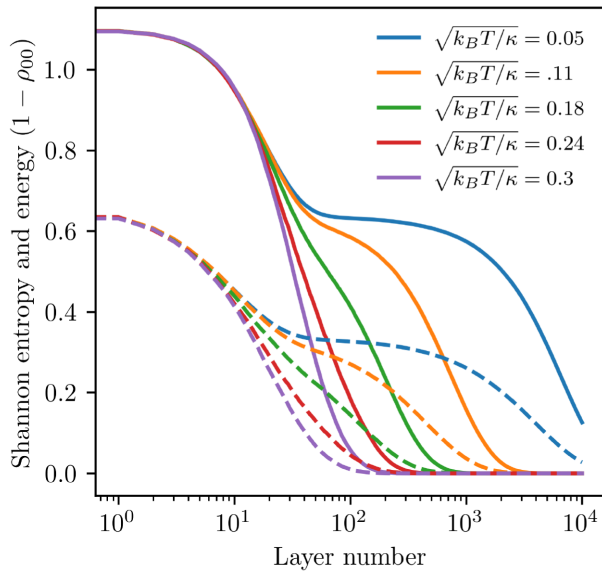


FIG. 9. The time dependence of the Shannon entropy (solid lines) and the energy $1 - p_0$ (dashed lines). Both display plateaus at intermediate times, which are made flatter at lower temperatures. This is due to the difference in time scales between absorption of horizontally and vertically polarized light. Both functions are decreasing and their relative slopes are different before and after the plateau.

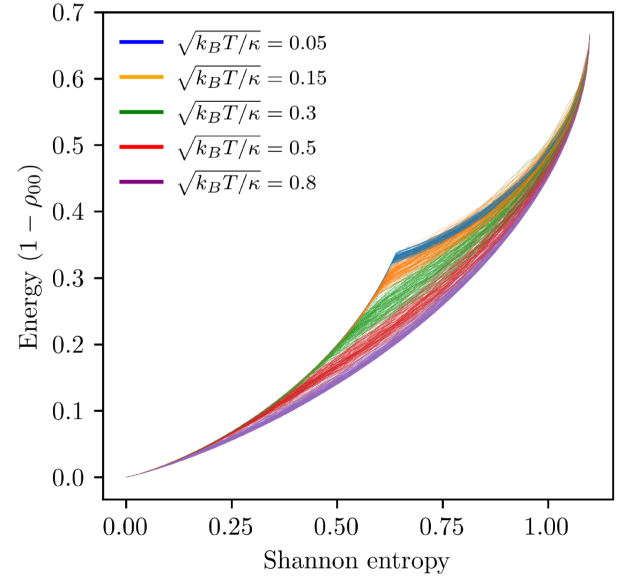


FIG. 10. The energy-entropy curve ensemble: 100 realizations of the polarization process are plotted with the same initial conditions but randomized transmission angles for the individual layers drawn from the Boltzmann distribution. The energy is monotonically increasing with the entropy but displays a discontinuity in its slope at zero temperature.

the plateaus appearing in Fig. 9 at low temperature. On the plateaus, both the entropy and the energy are nearly constant, although many layers of the polarizer are traversed. After the plateau, the relative slope of the energy and the entropy is different than what it was before and so a discontinuity of the slope dE/ds appears when the energy and the Shannon entropy are plotted against each other.

V. TEMPERATURE-DEPENDENT QUANTUM ERASER

We conclude the analysis with an experimentally testable consequence of our findings. We develop a theoretical model for the effect of temperature on the evolution of a single-photon state through a polarizing medium and our model predicts that at higher temperature there is enhanced decoherence. We now propose an experimental test of this, which is a modified quantum eraser experiment where the linear polarizer used to measure the polarization of one of the photons is in contact with a heat reservoir at temperature T . In the quantum eraser experiment [65–68,91,92], there are two photons, called the signal and idler photons. The signal photon may be either horizontally or vertically polarized or it may be absorbed by the polarizer so that it lives in a three-dimensional Hilbert space spanned by the vectors $|0\rangle$, $|h\rangle$, and $|v\rangle$. The idler photon may be either horizontally or vertically polarized and it may go down path 1 or path 2 of the interferometer, so it lives in a four-dimensional Hilbert space spanned by the

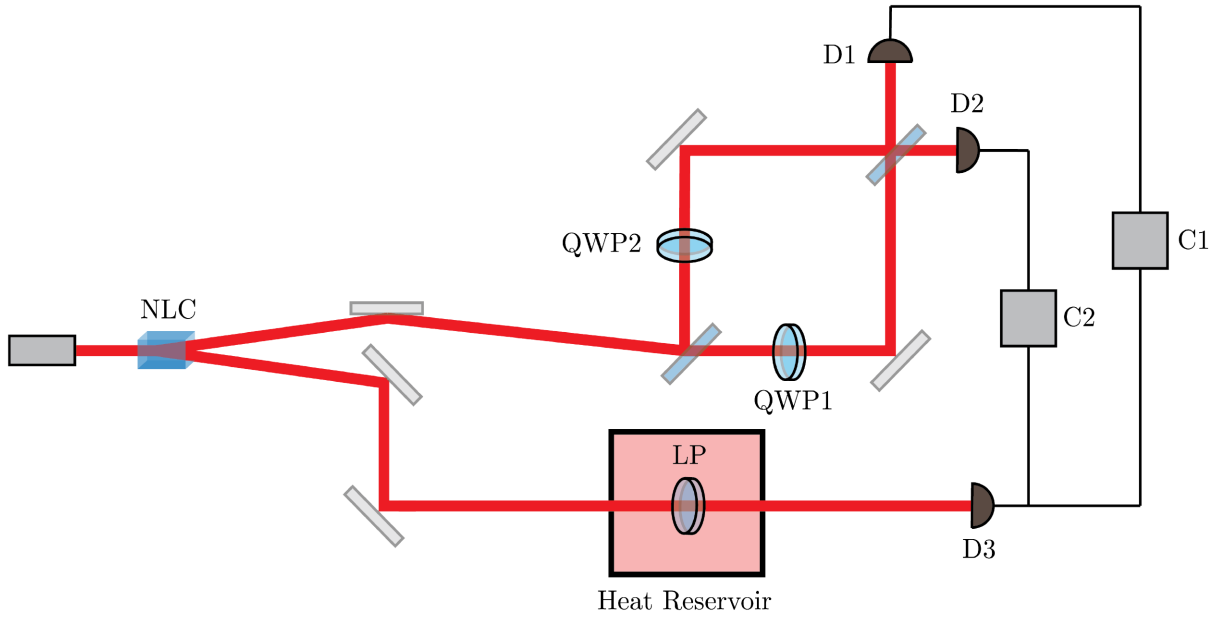


FIG. 11. The setup for the temperature-dependent quantum eraser experiment. NLC, nonlinear crystal; QWP1, QWP2, quarter-wave plates 1 and 2; LP, linear polarizer; D1, D2, D3, detectors 1–3; C1, C2, coincidence counters 1 and 2.

vectors $|h1\rangle$, $|v1\rangle$, $|h2\rangle$, and $|v2\rangle$. Therefore, the state of the two photons together belongs to a 12-dimensional Hilbert space spanned by the following states:

$$\begin{aligned} &|0h1\rangle, |hh1\rangle, |vh1\rangle, |0v1\rangle, |hv1\rangle, |vv1\rangle, \\ &|0h2\rangle, |hh2\rangle, |vh2\rangle, |0v2\rangle, |hv2\rangle, |vv2\rangle. \end{aligned} \quad (57)$$

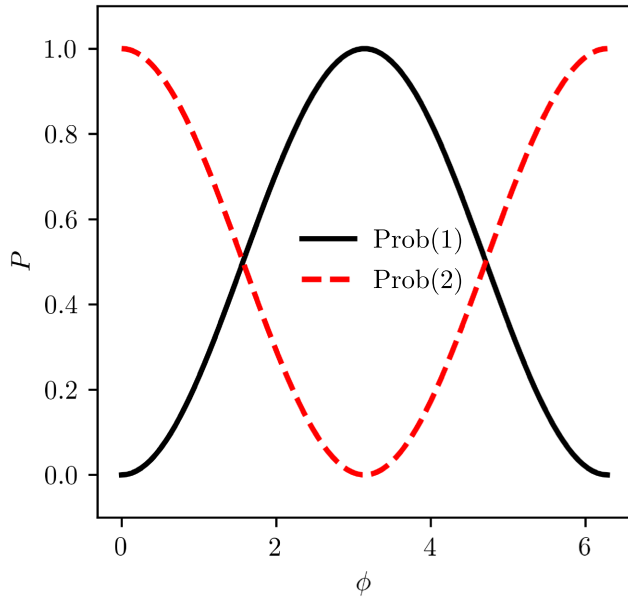


FIG. 12. The probability of the photon exiting each port as a function of the relative phase difference for the two arms in the unmarked case.

These states can be expressed as $|ijk\rangle$, where $i \in \{0, h, v\}$, $j \in \{h, v\}$, and $k \in \{1, 2\}$. Then, in general, we have a density matrix of the form

$$\sigma = \sum_{ijk} c_{ijk} |ijk\rangle \langle i'j'k'|. \quad (58)$$

The full density matrix can be written as a 4×4 array of 3×3 submatrices, where the indices in the 4×4 array correspond to the idler photon and the indices of each submatrix correspond to the signal photon:

$$\sigma = \begin{pmatrix} \rho_{v1,v1} & \rho_{v1,h1} & \rho_{v1,v2} & \rho_{v1,h2} \\ \rho_{h1,v1} & \rho_{h1,h1} & \rho_{h1,v2} & \rho_{h1,h2} \\ \rho_{v2,v1} & \rho_{v2,h1} & \rho_{v2,v2} & \rho_{v2,h2} \\ \rho_{h2,v1} & \rho_{h2,h1} & \rho_{h2,v2} & \rho_{h2,h2} \end{pmatrix}. \quad (59)$$

To evolve the density matrix forward by one step, we use Eq. (41). This gives

$$\sigma' = G_\theta(\sigma) = \begin{pmatrix} F_\theta(\rho_{v1,v1}) & \dots & F_\theta(\rho_{v1,h2}) \\ F_\theta(\rho_{h2,v1}) & \dots & F_\theta(\rho_{h2,h2}) \end{pmatrix}. \quad (60)$$

The initial condition for the quantum eraser experiment is a Bell state in the polarization basis for the two photons:

$$|\psi_0\rangle = \frac{1}{\sqrt{2}}(|hh1\rangle + |vv1\rangle). \quad (61)$$

First, a beam splitter is applied to the idler photon. There are two distinct configurations for the interferometer, one

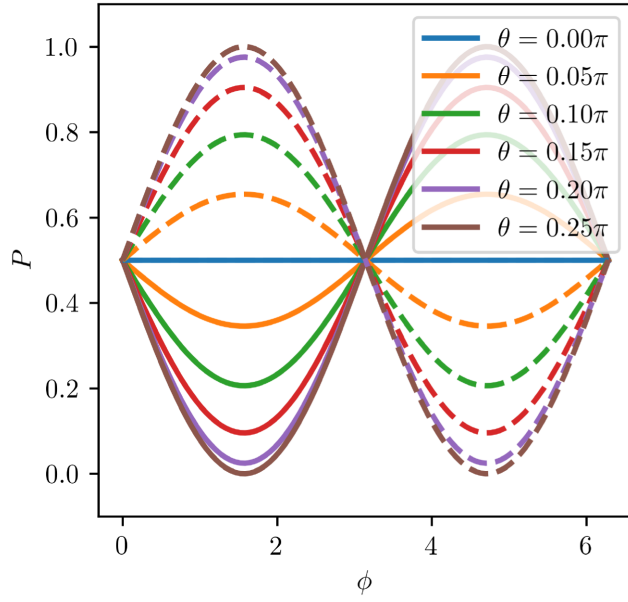


FIG. 13. The probability of the photon exiting each port as a function of the relative phase difference for the two arms in the marked case, with a measurement made on the signal photon by an LP at angle θ from the vertical.

in which the paths are “marked” and another in which the paths “unmarked.” For the marked configuration, there is a quarter-wave plate (QWP) in each path of the interferometer (see Fig. 11). One of the QWPs is at an angle of $\pi/4$ rad and the other at an angle of $-\pi/4$ rad. For the unmarked configuration, there are no QWPs. First, we simulate what happens in the unmarked configuration when there is no measurement made on the signal photon and recover the standard result of a simple Mach-Zehnder interferometer experiment (see Fig. 12) [93].

In the marked configuration, again with no measurement made on the signal photon, there is no interference pattern and the photon is detected by detectors 1 and 2 with equal probability. We then make a measurement on the signal photon with a linear polarizer at an angle θ from the vertical, resulting in a restoration of the interference pattern. We see that the interference pattern is gone when $\theta = 0$ and is completely restored for $\theta = \pi/4$, which is the main result of the traditional quantum eraser experiment (see Fig. 13). The variation in the interference pattern is most pronounced at a path phase difference of $\phi = \pi/2$.

We see from Fig. 14 that the effect of quantum erasing is temperature dependent. In particular, as the temperature is increased, the ability of the polarizer to restore interference is suppressed and eventually goes away entirely. While this phenomenon is explainable in greater detail when our model is solved analytically, we put forward the following interpretation based on our numerical results. The temperature-dependent erasing effect can be understood by reference to the enhanced decoherence at higher

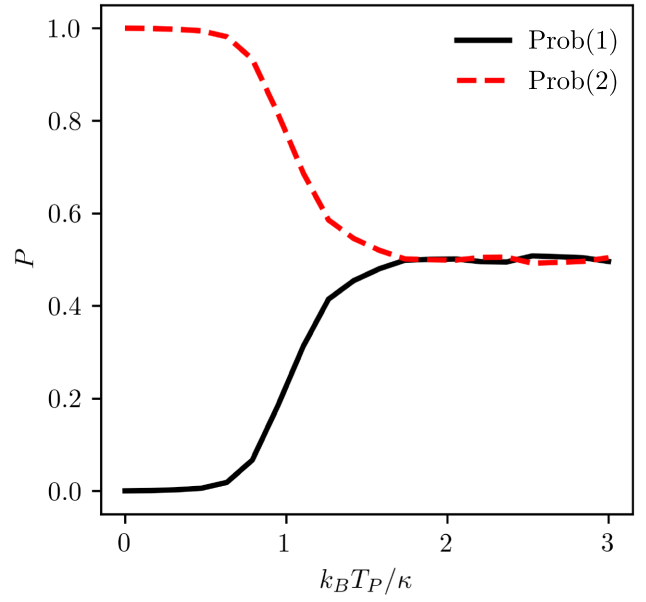


FIG. 14. The probability of the photon exiting each port as a function of temperature, with a relative phase of $\pi/2$ between the paths. Ensemble average of 1000 realizations.

temperature in our model, as seen in Fig. 8. The effects of decoherence cause the photon state to become diagonal in the measurement basis very quickly, much earlier than the time at which the populations reach their asymptotic values, which can be noted by comparing Figs. 8 and 7. This decoherence is a result of the mode in which the photon propagates becoming entangled with the modes in the environment with which it interacts through the repeated-interaction scheme and, as is well known, it cannot be maximally entangled with the other photon after becoming entangled with its environment due to entanglement monogamy [94]. Thus, the photons have effectively become disentangled before the measurement takes place, so the quantum erasing effect is suppressed.

VI. CONCLUDING REMARKS

Our analysis provides insight into the (quantum) thermodynamics of linear polarizers; we give explicit forms of Landauer’s principle for both absorbing linear polarizers and PBSs, which are listed in Table I. We also develop a formalism that incorporates the thermal energy contained in mechanical degrees of freedom of a polarizer and use this model to investigate the time-dependent dynamics of the polarization process. We provide a qualitative description of the dependence of this process on temperature and propose an experiment to test the temperature dependence of decoherence via a quantum eraser apparatus.

Some questions, which warrant further analysis, are left unanswered. A full solution of the master equation derived for the quantum absorbing polarizer, even in the

TABLE I. Statements of Landauer's principle given in the text, assumptions used in their derivation, and the relevant entropic quantities. Equation (46) is a preexisting result for collision models in general [11], which applies to the noisy-polarizer model given here.

Setting or device	Assumptions	Entropy type	Statement	Equation
Classical ALP	Final thermal state Finite energy No work reservoir	Differential Shannon	$Q \geq k_B T (e^{-\Delta s} - 1)$	(7)
Classical ALP	Final thermal state Finite energy No work reservoir	Differential Shannon	$\dot{d}Q \geq k_B T (-ds)$	(8)
Quantum ALP	Final thermal state Finite energy No work reservoir	Wigner	$Q \geq \frac{\hbar\omega}{2} \coth\left(\frac{\hbar\omega}{2k_B T}\right) (e^{-\Delta s_W} - 1)$	(19)
Quantum ALP	Final thermal state Finite energy No work reservoir	Wigner	$\dot{d}Q \geq \coth\left(\frac{\hbar\omega}{2k_B T}\right) (-ds_W)$	(20)
Semiclassical PBS	Initially unpolarized light Nonrelativistic PBS speed PBS momentum Boltzmann distributed Macroscopic PBS size Reflected photons eventually inaccessible	Shannon	$\dot{d}Q \geq \frac{\hbar^2 \omega^2}{2m^2 c^4} k_B T (-ds)$	(25)
Quantum PBS	Initially unpolarized light System-bath correlations eventually inaccessible Information-bearing degree of freedom globally conserved	Purity	$-\delta P \geq \frac{1}{N^{2N}} \left(1 - 2\sqrt{2}\epsilon\right)^2$	(30)
Noisy quantum ALP	Valid collision-model description $k_B T \ll \hbar\omega$	Von Neumann	$\dot{d}Q \geq k_B T (-ds)$	(46)

low-temperature limit and the single-photon subspace, is lacking. We also have not yet written a master equation that is valid when $k_B T$ is on the order of at least $\hbar\omega$. Answering these and other questions will provide guidance for the optimal control of optical polarization states. This is expected to be a particularly challenging task when $k_B T$ is nearly of the order of $\hbar\omega$, since environmental noise then becomes significant. Therefore, we hope to extend our results, with special attention paid to deriving a master equation valid in the high-temperature limit. It is then desirable to find bounds on the minimum dissipation required to perform various tasks in such an environment, including the version of Landauer's principle in Eq. (46). Another important direction for future work is to understand the implications of the effects that we describe, including temperature-dependent decoherence (as shown in Fig. 8), to definite applications in quantum communication.

ACKNOWLEDGMENTS

We would like to thank Todd Pittman, Alejandro Rodriguez Perez, Steve Campbell, and Pat Eblen

for enlighting discussions. M.A. gratefully acknowledges support from Harry Shaw of NASA Goddard Space Flight Center. N.M.M. acknowledges support from the Air Force Office of Scientific Research (AFOSR) (Grants No. FA2386-21-1-4081, No. FA9550-19-1-0272, and No. FA9550-23-1-0034) and the Army Research Office (ARO) (Grants No. W911NF2210247 and No. W911NF2010013). S.D. acknowledges support from the John Templeton Foundation under Grant No. 62422.

APPENDIX A: DERIVATION OF CLASSICAL LANDAUER'S PRINCIPLE

Recall that for a random vector of dimension D and with covariance matrix Σ , the entropy is upper bounded by that of the normal distribution [95,96],

$$s[f] \leq \frac{1}{2} \ln \left((2\pi e)^D |\Sigma| \right). \quad (\text{A1})$$

We regard f_α as a bivariate distribution over both the real and imaginary parts of α_v . Note that, in general, $\sqrt{|\Sigma|} \leq$

$\langle |\alpha_v|^2 \rangle / 2$, so

$$s[f_\alpha] \leq \ln(\pi e \langle |\alpha_v|^2 \rangle) = \ln\left(\frac{2e\pi E}{V\epsilon_0 E_{0\omega}^2}\right). \quad (\text{A2})$$

We assume that after the light has passed through the polarizer, it is in a thermal distribution with temperature T_P , which is associated with the polarizer itself. Therefore, the energy is $E' = k_B T$ and the entropy is

$$s[f'_\alpha] = \ln\left(\frac{2e\pi E'}{V\epsilon_0 E_{0\omega}^2}\right). \quad (\text{A3})$$

Consequently, the decrease in the Shannon entropy is at most

$$-\Delta s \leq \ln\left(\frac{2e\pi E}{V\epsilon_0 E_{0\omega}^2}\right) - \ln\left(\frac{2e\pi E'}{V\epsilon_0 E_{0\omega}^2}\right) = \ln\left(\frac{E}{E'}\right). \quad (\text{A4})$$

Since there is no work reservoir, all lost energy is dissipated as heat and we have

$$Q = E - E' = E' \left(\frac{E}{E'} - 1\right). \quad (\text{A5})$$

The use of $E' = k_B T_P$ and the upper bound on Δs then gives

$$Q \geq k_B T_P (e^{-\Delta s} - 1). \quad (\text{A6})$$

APPENDIX B: DERIVATION OF QUANTUM LANDAUER'S PRINCIPLE

Again using Eq. (A1), we find that

$$s_{\text{WM}}[W] = s[f_q] + s[f_p] \leq \ln\left(2\pi e \sqrt{\langle q^2 \rangle \langle p^2 \rangle}\right). \quad (\text{B1})$$

Due to Eq. (12), this is bounded above by

$$s_{\text{WM}}[W] \leq \ln\left(\frac{2\pi e E}{\hbar\omega}\right). \quad (\text{B2})$$

We again assume that the light is in a thermal state after leaving the polarizer. The thermal state has Wigner function [97,98]

$$W(q, p) = \frac{\hbar\omega}{\pi E'} \exp\left(-\frac{\hbar\omega(q^2 + p^2)}{2E'}\right), \quad (\text{B3})$$

where E' is given by

$$E'(T) = \hbar\omega \left(\frac{1}{\exp(\hbar\omega/k_B T) - 1} + \frac{1}{2} \right) \quad (\text{B4})$$

or, alternatively,

$$E'(T) = \frac{\hbar\omega}{2} \coth\left(\frac{\hbar\omega}{2k_B T}\right). \quad (\text{B5})$$

Since the thermal Wigner function given in Eq. (B3) is positive, the final Wigner entropy $s_W[W']$ is defined and is given by

$$s_W[W'] = \ln\left(\frac{2\pi e E'}{\hbar\omega}\right). \quad (\text{B6})$$

We can write

$$-\Delta s_W \leq s_{\text{WM}}[W] - s_W[W'] \leq \ln\left(\frac{E}{E'}\right). \quad (\text{B7})$$

We once again equate the heat to the lost energy:

$$Q = E' \left(\frac{E}{E'} - 1\right) \quad (\text{B8})$$

and hence

$$Q \geq \frac{\hbar\omega}{2} \coth\left(\frac{\hbar\omega}{2k_B T}\right) (e^{-\Delta s_W} - 1). \quad (\text{B9})$$

APPENDIX C: MINIMAL DISSIPATION FOR THE SEMICLASSICAL PBS

Let \hat{n} be the unit vector that is perpendicular to the PBS surface and is pointing *into* the bulk. The PBS and the photon have momenta \mathbf{p}_b and \mathbf{p} , respectively, in the laboratory frame. We define $p_{bn} = \hat{n} \cdot \mathbf{p}_b$ and $p_n = \hat{n} \cdot \mathbf{p}$ as the inward normal components of \mathbf{p}_b and \mathbf{p} . Using a Lorentz transformation, this component of the momentum of the photon in the rest frame of the PBS is then [99]

$$p_n^{(\text{PBS})} = \gamma(p_n - \hbar\omega p_{bn}/mc^2), \quad (\text{C1})$$

where γ is the Lorentz factor and ω is the frequency in the laboratory frame. Because the PBS momentum is nonrelativistic, we set $\gamma = 1$. We assume that in the rest frame of the PBS, the angle of reflection of the photon is the same as the angle of incidence, although this is only approximately true due to the transfer of energy from the photon to the PBS. That is, we set

$$p_n'^{(\text{PBS})} = -p_n^{(\text{PBS})}, \quad (\text{C2})$$

which is a good approximation when the PBS mass is macroscopic. Thus, in the laboratory frame, the momentum of the photon after the collision differs from its initial momentum by an amount

$$\delta p_n = p_n' - p_n = -2p_n + 2\hbar\omega p_{bn}/mc^2. \quad (\text{C3})$$

To ensure that a reflected photon can be distinguished from a transmitted photon, the difference in momentum

of the two paths should be greater than the uncertainty in momentum of the reflected photon, i.e.,

$$|\langle \delta p_n \rangle| \geq \sigma[\delta p_n]. \quad (\text{C4})$$

This condition is, in effect, a restriction on the statistical distance (as defined by Wootters [100]) between the momenta of the transmitted and reflected photons. And so from Eq. (C3) and the fact that $\sigma[p_n] = 0$, we have

$$|\delta p_n| \geq 2\hbar\omega\sigma[p_{bn}]/mc^2. \quad (\text{C5})$$

Because the PBS is at finite temperature T , we assume that its momentum is initially given by the canonical distribution

$$p_{bn} \sim \mathcal{N}(0, mk_B T) \quad (\text{C6})$$

and therefore

$$|\delta p_n| \geq \frac{2\hbar\omega}{c^2} \sqrt{\frac{k_B T}{m}}. \quad (\text{C7})$$

Next, note that for momentum to be conserved, the momentum of the PBS must also change by an amount $\delta p_{bn} = -\delta p_n$. In our convention, δp_{bn} is positive by definition, so

$$\delta p_{bn} \geq \frac{2\hbar\omega}{c^2} \sqrt{\frac{k_B T}{m}}. \quad (\text{C8})$$

Many photons are incident on the device, one after another. For each photon, the initial momentum p_n is the same and so δp_{bn} is very nearly the same for each reflected photon; hence we treat it as constant. We assume that each photon is vertically polarized with probability 1/2 and horizontally polarized with probability 1/2. So with probability 1/2, p_{bn} is increased by δp_{bn} as each photon passes. Therefore, after N photons have passed, the total change in the momentum of the PBS is given by a binomial distribution:

$$\frac{p_{bn}(t) - p_{bn}(0)}{\delta p_{bn}} \sim B(N, 1/2). \quad (\text{C9})$$

By the de Moivre–Laplace theorem [101], for large N , the distribution approaches a Gaussian with variance $\sigma^2 = N/4$. Therefore,

$$\sigma^2[p_{bn}(t) - p_{bn}(0)] = \delta p_{bn}^2 N/4. \quad (\text{C10})$$

Recall that the sum of two Gaussian random variables is Gaussian, with variance equal to the sum of the variances

of the two original distribution. Use of the variance of $p_{bn}(0)$ then gives

$$\sigma^2[p_{bn}(t)] = \delta p_{bn}^2 N/4 + mk_B T. \quad (\text{C11})$$

Then, using the formula for the Shannon entropy of a Gaussian, we have

$$s(t) - s(0) = \frac{1}{2} \ln \left(\frac{\delta p_{bn}^2 N/4 + mk_B T}{mk_B T} \right) \quad (\text{C12})$$

$$s(t) - s(0) \geq \frac{1}{2} \ln \left(\frac{\hbar^2 \omega^2}{m^2 c^4} N + 1 \right). \quad (\text{C13})$$

Our approximation is only valid for $\hbar\omega \ll mc^2$, and in this limit we have

$$s(t) - s(0) \geq \frac{1}{2} \frac{\hbar^2 \omega^2}{m^2 c^4} N. \quad (\text{C14})$$

After many photons have passed, p_n is in an equilibrium distribution, so we can equate the Shannon entropy with the thermal entropy. Then, the heat dissipated as a single photon passes is

$$Q \geq \frac{\hbar^2 \omega^2}{2m^2 c^4} k_B T. \quad (\text{C15})$$

The information carried by the photon is 1 bit, as per our assumption, so we may write this as

$$-dQ \geq \frac{\hbar^2 \omega^2}{2m^2 c^4} k_B T (-ds). \quad (\text{C16})$$

APPENDIX D: MINIMAL LOSS OF PURITY FOR QUANTUM PBS

The joint state of the system and the bath is acted on by a unitary operator U . We define the quantum state

$$\rho_B^i = \text{tr}_S \{ U[|i0\rangle \langle i0| \otimes \rho_B] U^\dagger \} \quad (\text{D1})$$

and

$$\rho_S^i = \text{tr}_B \{ U[|i0\rangle \langle i0| \otimes \rho_B] U^\dagger \}, \quad (\text{D2})$$

where $i \in \{0, 1\}$. Therefore, we write

$$\rho_B' = \frac{1}{2} (\rho_B^0 + \rho_B^1). \quad (\text{D3})$$

Now, we suppose that the bath is composed of N qubits. For conservation of angular momentum to hold, we require

that

$$\begin{aligned} \text{tr} \left\{ \rho_B^i \sum_{j=1}^N Z_B^j \right\} + \text{tr} \{ \rho_S^i (Z_S^1 + Z_S^2) \} = \\ \text{tr} \left\{ \rho_B \sum_{j=1}^N Z_B^j \right\} + \text{tr} \{ |i0\rangle \langle i0| (Z_S^1 + Z_S^2) \}, \end{aligned} \quad (\text{D4})$$

where Z is the Pauli- Z matrix. The noisy CNOT is implemented on the system qubits within accuracy ϵ , meaning

$$\sqrt{\text{tr} \{ (\rho'_S - U_{\text{CN}} \rho_S U_{\text{CN}}^\dagger)^2 \}} \leq \epsilon. \quad (\text{D5})$$

Employing the Cauchy-Schwarz inequality, we obtain

$$\begin{aligned} |\text{tr} \{ (\rho'_S - U_{\text{CN}} \rho_S U_{\text{CN}}^\dagger) (Z_S^1 + Z_S^2) \}| \leq \\ \epsilon \sqrt{\text{tr} \{ (Z_1 + Z_2)^2 \}} = 2\sqrt{2}\epsilon \end{aligned} \quad (\text{D6})$$

and hence

$$|\text{tr} \{ \rho_S^i (Z_S^1 + Z_S^2) \} - 2(-1)^i| \leq 2\sqrt{2}\epsilon \quad (\text{D7})$$

and

$$\text{tr} \{ |i0\rangle \langle i0| (Z_S^1 + Z_S^2) \} = (-1)^i - 1. \quad (\text{D8})$$

Finally, we can then write

$$\left| \text{tr} \left\{ (\rho_B^i - \rho_B) \sum_j Z_B^j \right\} - [-1 - (-1)^i] \right| \leq 2\sqrt{2}\epsilon, \quad (\text{D9})$$

which further leads to

$$\text{tr} \left\{ (\rho_B^1 - \rho_B^0) \sum_j Z_B^j \right\} \geq 2 - 4\sqrt{2}\epsilon. \quad (\text{D10})$$

Thus, the purity of the final state ρ'_B is

$$\text{tr} \{ \rho_B'^2 \} = \frac{1}{4} (\text{tr} \{ (\rho_B^0)^2 \} + \text{tr} \{ (\rho_B^1)^2 \} + 2\text{tr} \{ \rho_B^0 \rho_B^1 \}). \quad (\text{D11})$$

Note that the last term can also be expressed as

$$\begin{aligned} 2\text{tr} \{ \rho_B^0 \rho_B^1 \} &= \text{tr} \{ (\rho_B^0)^2 \} + \text{tr} \{ (\rho_B^1)^2 \} \\ &\quad - \text{tr} \{ (\rho_B^1 - \rho_B^0)^2 \}. \end{aligned} \quad (\text{D12})$$

Now, since the purity of the states ρ_B^0 and ρ_B^1 cannot exceed the purity of ρ_B , we have

$$2\text{tr} \{ \rho_B^0 \rho_B^1 \} \leq 2\text{tr} \{ \rho_B^2 \} - \text{tr} \{ (\rho_B^1 - \rho_B^0)^2 \}. \quad (\text{D13})$$

Using the Cauchy-Schwarz inequality again, we obtain

$$\begin{aligned} \text{tr} \left\{ (\rho_B^1 - \rho_B^0) \sum_{j=1}^N Z_B^j \right\}^2 \leq \\ \text{tr} \{ (\rho_B^1 - \rho_B^0)^2 \} \text{tr} \left\{ \left(\sum_{j=1}^N Z_B^j \right)^2 \right\} \end{aligned} \quad (\text{D14})$$

and with $\text{tr} \{ Z_i Z_j \} = 0$ for $i \neq j$, we can have

$$\text{tr} \left\{ \left(\sum_{j=1}^N Z_j \right)^2 \right\} = \text{tr} \left\{ \sum_{j=1}^N Z_j^2 \right\} = N2^N. \quad (\text{D15})$$

Collecting expressions, we can further write

$$\begin{aligned} \text{tr} \{ (\rho_B^1 - \rho_B^0)^2 \} &\geq \frac{1}{N2^N} \text{tr} \left\{ (\rho_B^1 - \rho_B^0) \sum_j Z_B^j \right\}^2 \\ &\geq \frac{(2 - 4\sqrt{2}\epsilon)^2}{N2^N} \end{aligned} \quad (\text{D16})$$

and, finally,

$$2\text{tr} \{ \rho_B^0 \rho_B^1 \} \leq 2\text{tr} \{ \rho_B^2 \} - \frac{(2 - 4\sqrt{2}\epsilon)^2}{N2^N}, \quad (\text{D17})$$

which we rewrite (as in the main text) as

$$\text{tr} \{ \rho_B'^2 \} \leq \text{tr} \{ \rho_B^2 \} - \frac{1}{N2^N} (1 - 2\sqrt{2}\epsilon)^2. \quad (\text{D18})$$

APPENDIX E: DERIVATION OF MODIFIED COMMUTATION RELATION

Consider the case where a PBS is at an unknown angle θ , with some probability density $p(\theta)$. If the state of the two input modes is given some density matrix $\sigma_0 = \rho_0 \otimes \eta_0$, then the output density matrix is

$$\sigma_1 = \int_{-\infty}^{\infty} d\theta p(\theta) U_\theta \sigma_0 U_\theta^\dagger = \mathcal{E}(\sigma_0), \quad (\text{E1})$$

where we define \mathcal{E} as the quantum channel that propagates the density matrix in the Schrödinger picture. There is an adjoint map \mathcal{E}^\dagger that can be used to propagate operators in

the Heisenberg picture and that satisfies [102]

$$\text{tr} \{ \rho \mathcal{E}^\dagger(X) \} = \text{tr} \{ \mathcal{E}(\rho) X \}, \quad (\text{E2})$$

for all density matrices ρ and operators X . In fact, it is easily seen that \mathcal{E}^\dagger is given by

$$\mathcal{E}^\dagger(X) = \int_{-\infty}^{\infty} d\theta f(\theta) U_\theta^\dagger X U_\theta. \quad (\text{E3})$$

Then, using Eq. (31), we see that the adjoint map acting on the annihilation operators x_i can be expressed as

$$\mathcal{E}^\dagger(x_i) = (\bar{S}\mathbf{x})_i, \quad (\text{E4})$$

where we define the ensemble-averaged scattering matrix as

$$\bar{S} = \int_{-\infty}^{\infty} d\theta f(\theta) S_\theta. \quad (\text{E5})$$

Note that the evolved operators $\mathcal{E}(x_i)$ no longer necessarily obey the standard Dirac commutation relation, since \bar{J} need not be unitary. While we can evaluate expectation values using Eq. (E2), we cannot build new operators or states using the evolved operators. However, many useful operators are expressed in terms of products of annihilation operators. We consider the class of operators that can be

written as

$$X = \sum_{ij} X_{ij} x_i^\dagger x_j. \quad (\text{E6})$$

To see how such an operator evolves under these dynamics, we first note that

$$U_\theta^\dagger x_i^\dagger x_j U_\theta = \sum_k S_{\theta ik}^* x_k^\dagger \sum_\ell S_{\theta j \ell} x_\ell = \sum_{k\ell} S_{k\ell}^{ij}(\theta) x_k^\dagger x_\ell, \quad (\text{E7})$$

where we define

$$S_{k\ell}^{ij}(\theta) = S_{\theta ik}^* S_{\theta j \ell}. \quad (\text{E8})$$

Therefore, by Eq. (E3), we have

$$\mathcal{E}^\dagger(X) = \sum_{ijkl} X_{ij} \bar{S}_{k\ell}^{ij} x_k^\dagger x_\ell, \quad (\text{E9})$$

where

$$\bar{S}_{k\ell}^{ij} = \int_{-\infty}^{\infty} d\theta p(\theta) S_{k\ell}^{ij}(\theta). \quad (\text{E10})$$

We now assume that $f(\theta)$ is Gaussian, with some temperature T :

$$f(\theta) = \frac{1}{\sqrt{2\pi k_B T/\kappa}} \exp\left(-\frac{1}{2} \frac{\theta^2}{k_B T/\kappa}\right). \quad (\text{E11})$$

Then, evaluating Eq. (E5), we find that

$$\bar{S} = \begin{pmatrix} 1 - (1-t)\chi & 0 & r\chi & 0 \\ 0 & t + (1-t)\chi & 0 & r - r\chi \\ -r\chi & 0 & 1 - (1-t)\chi & 0 \\ 0 & r\chi - r & 0 & t + (1-t)\chi \end{pmatrix}, \quad (\text{E12})$$

where $\chi = 1/2 (1 - \exp(-2k_B T/\kappa))$. We can then express the primed annihilation operators as

$$a'_h = (1 - (1-t)\chi) a_h - r\chi b_h \quad (\text{E13})$$

and

$$a'_v = (t + (1-t)\chi) a_v + r(\chi - 1) b_v. \quad (\text{E14})$$

Note that χ is a monotonically increasing function of temperature and $\chi = 0$ at $T = 0$ and hence Eqs. (E13) and (E14) clearly show the influence on increasing temperature on the propagation of the annihilation operators. For

zero temperature, we have

$$\lim_{T \rightarrow 0} a'_h = a_h \quad \text{and} \quad \lim_{T \rightarrow 0} a'_v = t a_v - r b_v, \quad (\text{E15})$$

meaning that the model behaves as a PBS at definite angle, as expected. In the limit of infinite temperature $\chi \rightarrow 1/2$ and we find that

$$\lim_{T \rightarrow \infty} a'_h = \frac{1+t}{2} a_h - \frac{r}{2} b_h \quad (\text{E16})$$

and

$$\lim_{T \rightarrow \infty} a'_v = \frac{1+t}{2} a_v - \frac{r}{2} b_v, \quad (\text{E17})$$

meaning that horizontally polarized and vertically polarized light are not distinguished by the device. The primed

annihilation operators do not obey the standard commutation relations. Instead, we find that

$$[a'_h, a'^{\dagger}_h] = [a'_v, a'^{\dagger}_v] = 1 - 2(1 - t)(\chi - \chi^2). \quad (\text{E18})$$

APPENDIX F: CONSTRUCTION OF THE EVOLUTION OPERATOR

In this appendix, we show that the two treatments that we give in the Heisenberg and the Schrödinger picture are, in fact, equivalent. This formulation is not a new result but we include it for convenience (for similar calculations, see, e.g., Refs. [103,104]). Recall that the evolution operator is obtained as follows, for $t = 1$:

$$U(t) = \exp \left(t \sum_{ij} \langle i | \ln(S) | j \rangle a_i^{\dagger} a_j \right), \quad (\text{F1})$$

where S is the unitary scattering matrix. Then,

$$\partial_t a'_k = (\partial_t U^{\dagger}) a_k U + U^{\dagger} a_k (\partial_t U) \quad (\text{F2})$$

and

$$\partial_t a'_k = U^{\dagger} \sum_{ij} \langle j | \ln(S)^{\dagger} | i \rangle a_j^{\dagger} a_i a_k U + U^{\dagger} \sum_{ij} \langle i | \ln(S) | j \rangle a_k a_i^{\dagger} a_j U. \quad (\text{F3})$$

Since S is unitary, $\ln(S)$ is anti-Hermitian. Using this fact and interchanging i and j in the first summation, we obtain

$$\partial_t a'_k = U^{\dagger} \left(- \sum_{ij} \langle i | \ln(S) | j \rangle a_i^{\dagger} a_j a_k + \sum_{ij} \langle i | \ln(S) | j \rangle a_k a_i^{\dagger} a_j \right) U \quad (\text{F4})$$

and

$$\partial_t a'_k = U^{\dagger} \sum_{ij} \langle i | \ln(S) | j \rangle [a_k, a_i^{\dagger} a_j] U = U^{\dagger} \sum_j \langle k | \ln(S) | j \rangle a_j U. \quad (\text{F5})$$

Thus, we have

$$\partial_t a'_k = \sum_j \langle k | \ln(S) | j \rangle a'_j. \quad (\text{F6})$$

The unique solution to this equation is

$$a'_k = \sum_{kj} \langle k | \exp(t \ln S) | j \rangle a'_j. \quad (\text{F7})$$

-
- [1] M. G. Raymer and C. Monroe, The US national quantum initiative, *Quantum Sci. Technol.* **4**, 020504 (2019).
 - [2] S. Deffner and S. Campbell, *Quantum Thermodynamics* (Morgan & Claypool Publishers, San Rafael, California, 2019).

-
- [3] J. M. R. Parrondo, J. M. Horowitz, and T. Sagawa, Thermodynamics of information, *Nat. Phys.* **11**, 131 (2015).
 - [4] R. Landauer, Irreversibility and heat generation in the computing process, *IBM J. Res. Dev.* **5**, 183 (1961).
 - [5] B. Piechocinska, Information erasure, *Phys. Rev. A* **61**, 062314 (2000).

- [6] S. Deffner and C. Jarzynski, Information Processing and the Second Law of Thermodynamics: An Inclusive, Hamiltonian Approach, *Phys. Rev. X* **3**, 041003 (2013).
- [7] A. B. Boyd and J. P. Crutchfield, Maxwell Demon Dynamics: Deterministic Chaos, the Szilard Map, and the Intelligence of Thermodynamic Systems, *Phys. Rev. Lett.* **116**, 190601 (2016).
- [8] A. B. Boyd, D. Mandal, and J. P. Crutchfield, Identifying functional thermodynamics in autonomous Maxwellian ratchets, *New J. Phys.* **18**, 023049 (2016).
- [9] A. B. Boyd, D. Mandal, and J. P. Crutchfield, Thermodynamics of Modularity: Structural Costs beyond the Landauer Bound, *Phys. Rev. X* **8**, 031036 (2018).
- [10] S. Hilt, S. Shabbir, J. Anders, and E. Lutz, Landauer's principle in the quantum regime, *Phys. Rev. E* **83**, 030102 (2011).
- [11] S. Lorenzo, R. McCloskey, F. Ciccarello, M. Paternostro, and G. Palma, Landauer's Principle in Multipartite Open Quantum System Dynamics, *Phys. Rev. Lett.* **115**, 120403 (2015).
- [12] T. Van Vu and K. Saito, Finite-Time Quantum Landauer Principle and Quantum Coherence, *Phys. Rev. Lett.* **128**, 010602 (2022).
- [13] J. Goold, M. Paternostro, and K. Modi, Nonequilibrium Quantum Landauer Principle, *Phys. Rev. Lett.* **114**, 060602 (2015).
- [14] A. Bérut, A. Arakelyan, A. Petrosyan, S. Ciliberto, R. Dillenschneider, and E. Lutz, Experimental verification of Landauer's principle linking information and thermodynamics, *Nature* **483**, 187 (2012).
- [15] O. J. E. Maroney, Generalizing Landauer's principle, *Phys. Rev. E* **79**, 031105 (2009).
- [16] J. D. Norton, Waiting for Landauer, *Stud. Hist. Philos. Sci. Part B: Stud. Hist. Philos. Mod. Phys.* **42**, 184 (2011).
- [17] O. Maroney, The (absence of a) relationship between thermodynamic and logical reversibility, *Stud. Hist. Philos. Sci. Part B: Stud. Hist. Philos. Mod. Phys.* **36**, 355 (2005).
- [18] B. Bylicka, M. Tukiainen, D. Chruściński, J. Piilo, and S. Maniscalco, Thermodynamic power of non-Markovianity, *Sci. Rep.* **6**, 27989 (2016).
- [19] M. Pezzutto, M. Paternostro, and Y. Omar, Implications of non-Markovian quantum dynamics for the Landauer bound, *New J. Phys.* **18**, 123018 (2016).
- [20] Q. Zhang, Z.-X. Man, and Y.-J. Xia, Non-Markovianity and the Landauer principle in composite thermal environments, *Phys. Rev. A* **103**, 032201 (2021).
- [21] H.-R. Hu, L. Li, J. Zou, and W.-M. Liu, Relation between non-Markovianity and Landauer's principle, *Phys. Rev. A* **105**, 062429 (2022).
- [22] Z.-X. Man, Y.-J. Xia, and R. Lo Franco, Validity of the Landauer principle and quantum memory effects via collisional models, *Phys. Rev. A* **99**, 042106 (2019).
- [23] H. J. Bremermann, in *Proceedings of the Fifth Berkeley Symposium on Mathematical Statistics and Probability, Volume 4: Biology and Problems of Health* (University of California Press, Berkeley, California, 1967), p. 15.
- [24] W. Heisenberg, Über den anschaulichen Inhalt der quantentheoretischen Kinematik und Mechanik, *Z. Phys.* **43**, 172 (1927).
- [25] J. D. Bekenstein, Energy Cost of Information Transfer, *Phys. Rev. Lett.* **46**, 623 (1981).
- [26] J. D. Bekenstein, Black holes and entropy, *Phys. Rev. D* **7**, 2333 (1973).
- [27] J. D. Bekenstein, Generalized second law of thermodynamics in black-hole physics, *Phys. Rev. D* **9**, 3292 (1974).
- [28] S. W. Hawking, Particle creation by black holes, *Commun. Math. Phys.* **43**, 199 (1975).
- [29] J. D. Bekenstein, Universal upper bound on the entropy-to-energy ratio for bounded systems, *Phys. Rev. D* **23**, 287 (1981).
- [30] J. D. Bekenstein and M. Schiffer, Quantum limitations on the storage and transmission of information, *Int. J. Mod. Phys. C* **1**, 355 (1990).
- [31] J. B. Pendry, Quantum limits to the flow of information and entropy, *J. Phys. A: Math. Gen.* **16**, 2161 (1983).
- [32] R. Landauer, Energy requirements in communication, *Appl. Phys. Lett.* **51**, 2056 (1987).
- [33] J. D. Bekenstein, Communication and energy, *Phys. Rev. A* **37**, 3437 (1988).
- [34] C. M. Caves and P. D. Drummond, Quantum limits on bosonic communication rates, *Rev. Mod. Phys.* **66**, 481 (1994).
- [35] M. P. Blencowe and V. Vitelli, Universal quantum limits on single-channel information, entropy, and heat flow, *Phys. Rev. A* **62**, 052104 (2000).
- [36] S. Lloyd, V. Giovannetti, and L. Maccone, Physical Limits to Communication, *Phys. Rev. Lett.* **93**, 100501 (2004).
- [37] P. Garbaczewski, Information dynamics in quantum theory, *Appl. Math. Inf. Sci.* **1**, 1 (2007).
- [38] G. Pei-Rong and L. Di, Upper bound for the time derivative of entropy for a stochastic dynamical system with double singularities driven by non-Gaussian noise, *Chin. Phys. B* **19**, 030520 (2010).
- [39] S. Deffner and E. Lutz, Generalized Clausius Inequality for Nonequilibrium Quantum Processes, *Phys. Rev. Lett.* **105**, 170402 (2010).
- [40] Y. Guo, W. Xu, H. Liu, D. Li, and L. Wang, Upper bound of time derivative of entropy for a dynamical system driven by quasimonochromatic noise, *Commun. Nonlinear Sci. Numer. Simul.* **16**, 522 (2011).
- [41] Y.-F. Guo and J.-G. Tan, Time evolution of information entropy for a stochastic system with double singularities driven by quasimonochromatic noise, *Chin. Phys. B* **21**, 120501 (2012).
- [42] R. Bousso, Universal Limit on Communication, *Phys. Rev. Lett.* **119**, 140501 (2017).
- [43] R. J. Lewis-Swan, A. Safavi-Naini, A. M. Kaufman, and A. M. Rey, Dynamics of quantum information, *Nat. Rev. Phys.* **1**, 627 (2019).
- [44] S. Deffner, Quantum speed limits and the maximal rate of information production, *Phys. Rev. Res.* **2**, 013161 (2020).
- [45] N. Gisin and R. Thew, Quantum communication, *Nat. Phot.* **1**, 165 (2007).
- [46] J. Chen, Review on quantum communication and quantum computation, *J. Phys.: Conf. Ser.* **1865**, 022008 (2021).
- [47] S. Wehner, D. Elkouss, and R. Hanson, Quantum Internet: A vision for the road ahead, *Science* **362**, eaam9288 (2018).

- [48] N. Gisin, G. Ribordy, W. Tittel, and H. Zbinden, Quantum cryptography, *Rev. Mod. Phys.* **74**, 145 (2002).
- [49] C.-Y. Lu, Y. Cao, C.-Z. Peng, and J.-W. Pan, Micius quantum experiments in space, *Rev. Mod. Phys.* **94**, 035001 (2022).
- [50] H.-J. Briegel, W. Dür, J. I. Cirac, and P. Zoller, Quantum Repeaters: The Role of Imperfect Local Operations in Quantum Communication, *Phys. Rev. Lett.* **81**, 5932 (1998).
- [51] W. J. Munro, K. Azuma, K. Tamaki, and K. Nemoto, Inside quantum repeaters, *IEEE J. Sel. Top. Quantum Electron.* **21**, 78 (2015).
- [52] L. Jiang, J. M. Taylor, N. Khaneja, and M. D. Lukin, Optimal approach to quantum communication using dynamic programming, *Proc. Natl. Acad. Sci. U.S.A.* **104**, 17291 (2007).
- [53] A. Auffèves, Quantum Technologies Need a Quantum Energy Initiative, *PRX Quantum* **3**, 020101 (2022).
- [54] L. Eldada, Optical communication components, *Rev. Sci. Instrum.* **75**, 575 (2004).
- [55] R. C. Jones, Ultimate performance of polarizers for visible light, *J. Opt. Soc. Am.* **52**, 747 (1962).
- [56] S. Im, E. Sim, and D. Kim, Microscale heat transfer and thermal extinction of a wire-grid polarizer, *Sci. Rep.* **8**, 14973 (2018).
- [57] B. Lounis and M. Orrit, Single-photon sources, *Rep. Prog. Phys.* **68**, 1129 (2005).
- [58] K. Edamatsu, Entangled photons: Generation, observation, and characterization, *Jpn. J. Appl. Phys.* **46**, 7175 (2007).
- [59] S. Takeuchi, Recent progress in single-photon and entangled-photon generation and applications, *Jpn. J. Appl. Phys.* **53**, 030101 (2014).
- [60] T. Konrad and A. Forbes, Quantum mechanics and classical light, *Contemp. Phys.* **60**, 1 (2019).
- [61] A. Kenfack and K. Życzkowski, Negativity of the Wigner function as an indicator of non-classicality, *J. Opt. B: Quantum Semiclass. Opt.* **6**, 396 (2004).
- [62] S. Campbell and B. Vacchini, Collision models in open system dynamics: A versatile tool for deeper insights?, *Europhys. Lett.* **133**, 60001 (2021).
- [63] S. Lorenzo, R. McCloskey, F. Ciccarello, M. Paternostro, and G. M. Palma, Landauer's Principle in Multipartite Open Quantum System Dynamics, *Phys. Rev. Lett.* **115**, 120403 (2015).
- [64] A. Aiello and J. P. Woerdman, Physical Bounds to the Entropy-Depolarization Relation in Random Light Scattering, *Phys. Rev. Lett.* **94**, 090406 (2005).
- [65] M. O. Scully and K. Drühl, Quantum eraser: A proposed photon correlation experiment concerning observation and "delayed choice" in quantum mechanics, *Phys. Rev. A* **25**, 2208 (1982).
- [66] Y.-H. Kim, R. Yu, S. P. Kulik, Y. Shih, and M. O. Scully, Delayed "Choice" Quantum Eraser, *Phys. Rev. Lett.* **84**, 1 (2000).
- [67] S. P. Walborn, M. O. Terra Cunha, S. Pádua, and C. H. Monken, Double-slit quantum eraser, *Phys. Rev. A* **65**, 033818 (2002).
- [68] K. Kang, Electronic Mach-Zehnder quantum eraser, *Phys. Rev. B* **75**, 125326 (2007).
- [69] C. H. Bennett, Notes on Landauer's principle, reversible computation, and Maxwell's demon, *Stud. Hist. Philos. Sci. Part B: Stud. Hist. Philos. Mod. Phys.* **34**, 501 (2003).
- [70] F. Bucholtz, J. V. Michalowicz, J. M. Nichols, and F. Bucholtz, *Handbook of Differential Entropy* (CRC Press, Taylor & Francis Group, Boca Raton, 2014).
- [71] G. Grynberg, A. Aspect, C. Fabre, and C. Cohen-Tannoudji, *Introduction to Quantum Optics: From the Semi-Classical Approach to Quantized Light* (Cambridge University Press, Cambridge, United Kingdom, 2010).
- [72] P. Ehrenfest, Welche Züge der Lichtquantenhypothese spielen in der Theorie der Wärmestrahlung eine wesentliche Rolle?, *Ann. Phys.* **341**, 91 (1911).
- [73] W. P. Schleich, *Quantum Optics in Phase Space* (John Wiley & Sons, Berlin, Germany, 2011).
- [74] Z. Van Herstraeten and N. J. Cerf, Quantum Wigner entropy, *Phys. Rev. A* **104**, 042211 (2021).
- [75] J. P. Santos, G. T. Landi, and M. Paternostro, Wigner Entropy Production Rate, *Phys. Rev. Lett.* **118**, 220601 (2017).
- [76] E. Witten, A mini-introduction to information theory, *Riv. Nuovo Cim.* **43**, 187 (2020).
- [77] H. Fearn and R. Loudon, Quantum theory of the lossless beam splitter, *Opt. Commun.* **64**, 485 (1987).
- [78] A. Aspect, From Huygens' waves to Einstein's photons: Weird light, *C.R. Phys.* **18**, 498 (2017).
- [79] R. Okamoto, H. F. Hofmann, S. Takeuchi, and K. Sasaki, Demonstration of an Optical Quantum Controlled-NOT Gate without Path Interference, *Phys. Rev. Lett.* **95**, 210506 (2005).
- [80] T. Karasawa, J. Gea-Banacloche, and M. Ozawa, Gate fidelity of arbitrary single-qubit gates constrained by conservation laws, *J. Phys. A: Math. Theor.* **42**, 225303 (2009).
- [81] M. Ozawa, Conservative Quantum Computing, *Phys. Rev. Lett.* **89**, 057902 (2002).
- [82] A. Touil, B. Yan, D. Girolami, S. Deffner, and W. H. Zurek, Eavesdropping on the Decohering Environment: Quantum Darwinism, Amplification, and the Origin of Objective Classical Reality, *Phys. Rev. Lett.* **128**, 010401 (2022).
- [83] D. Girolami, A. Touil, B. Yan, S. Deffner, and W. H. Zurek, Redundantly Amplified Information Suppresses Quantum Correlations in Many-Body Systems, *Phys. Rev. Lett.* **129**, 010401 (2022).
- [84] A. Touil, F. Anza, S. Deffner, and J. P. Crutchfield, Branching states as the emergent structure of a quantum universe, arXiv preprint [arXiv:2208.05497](https://arxiv.org/abs/2208.05497) (2022).
- [85] S. Cusumano, Quantum collision models: A beginner guide, *Entropy* **24**, 1258 (2022).
- [86] J. Rau, Relaxation phenomena in spin and harmonic oscillator systems, *Phys. Rev.* **129**, 1880 (1963).
- [87] M. A. Nielsen and I. L. Chuang, *Quantum Computation and Quantum Information* (Cambridge University Press, Cambridge, United Kingdom, 2010).
- [88] S. Takahashi, J. van Tol, C. C. Beedle, D. N. Hendrickson, L.-C. Brunel, and M. S. Sherwin, Coherent Manipulation and Decoherence of $S = 10$ Single-Molecule Magnets, *Phys. Rev. Lett.* **102**, 087603 (2009).

- [89] A. E. Hansen, A. Kristensen, S. Pedersen, C. B. Sørensen, and P. E. Lindelof, Mesoscopic decoherence in Aharonov-Bohm rings, *Phys. Rev. B* **64**, 045327 (2001).
- [90] P. Mohanty and R. A. Webb, Decoherence and quantum fluctuations, *Phys. Rev. B* **55**, R13452 (1997).
- [91] T. J. Herzog, P. G. Kwiat, H. Weinfurter, and A. Zeilinger, Complementarity and the Quantum Eraser, *Phys. Rev. Lett.* **75**, 3034 (1995).
- [92] T. Peng, H. Chen, Y. Shih, and M. O. Scully, Delayed-Choice Quantum Eraser with Thermal Light, *Phys. Rev. Lett.* **112**, 180401 (2014).
- [93] K. P. Zetie, S. F. Adams, and R. M. Tocknell, How does a Mach-Zehnder interferometer work?, *Phys. Educ.* **35**, 46 (2000).
- [94] D. Yang, A simple proof of monogamy of entanglement, *Phys. Lett. A* **360**, 249 (2006).
- [95] D. Dowson and A. Wragg, Maximum-entropy distributions having prescribed first and second moments (Corresp.), *IEEE Trans. Inf. Theory* **19**, 689 (1973).
- [96] H. W. Chung, B. M. Sadler, and A. O. Hero, Bounds on variance for unimodal distributions, *IEEE Trans. Inf. Theory* **63**, 6936 (2017).
- [97] N. Bhusal, Smart quantum technologies using photons (2021), [arXiv:2103.07081](https://arxiv.org/abs/2103.07081) [physics, physics:quant-ph].
- [98] T. Curtright, D. Fairlie, and C. Zachos, *A Concise Treatise on Quantum Mechanics in Phase Space* (World Scientific, Hackensack, New Jersey, 2014).
- [99] A. P. French, *Special Relativity* (CRC Press, London, United Kingdom, 2017), 1st ed.
- [100] W. K. Wootters, Statistical distance and Hilbert space, *Phys. Rev. D* **23**, 357 (1981).
- [101] E. W. Weisstein, De Moivre–Laplace theorem. From MathWorld—A Wolfram Web Resource. Date of access: October 10, 2022. <https://mathworld.wolfram.com/deMoivre-LaplaceTheorem.html>.
- [102] M. M. Wolf, *Quantum Channels & Operations Guided Tour* (Citeseer, 2012). <https://mediatum.ub.tum.de/doc/1701036/document.pdf>.
- [103] U. Leonhardt, *Essential Quantum Optics: From Quantum Measurements to Black Holes* (Cambridge University Press, Cambridge, United Kingdom, 2010), 1st ed.
- [104] U. Leonhardt, Quantum physics of simple optical instruments, *Rep. Prog. Phys.* **66**, 1207 (2003).